acta physica slovaca vol. 44 No. 6, 481 – 492 December 1994

DISPERSION RELATION ANALYSIS OF THE ELASTIC SCATTERING OF ALPHA-PARTICLES BY ^{40}Ca

W. Haider*, P. E. Hodgson
Nuclear Physics Laboratory, Department of Physics, University of Oxford, U. K.

Received 5 July 1994, revised 24 August 1994, accepted 24 August 1994

The differential cross-sections for the elastic scattering of alpha-particles by ^{40}Ca are analysed using the dispersion relation for optical model potentials with Saxon-Woods form factors. The dispersion relation gives rise to a real surface peaked term as a consequence of the empirical surface imaginary potential. Including this real surface term gives a consistant account of the data over the whole energy region.

1. Introduction

Optical model analyses of nucleon-nucleus scattering, particularly by Mahaux and collaborators, have shown that it is possible to fit the differential cross-section and polarisation data with potentials whose real and imaginary parts satisfy a dispersion relation. This enables the interaction between a nucleon and a nucleus to be treated in a unified way over the whole energy range from bound to scattering states, and shows the connection between the real and imaginary parts of the optical potential [1].

The dispersion relation should also be applicable to the interaction of composite particles, and some investigations have already shown that they can be used successfully to analyse alpha-particle scattering [2]. Several other studies have also shown that empirical potentials can be found that unify the bound state and scattering data for the interaction of alphaparticles with nuclei, particularly with ^{40}Ca [3].

The purpose of the present work is to make a full dispersion relation analysis of alpha-^{40}Ca elastic scattering data with the possibility of extending the alpha-particle potential to the bound state region. The nucleus ^{40}Ca was chosen because there is avaiable a large body of accurate elastic scattering data over the whole energy range.

Mahaux et al [2] applied the subtracted dispersion relation to the elastic scattering of alpha-particles by ^{16}O, ^{40}Ca and ^{58}Ni and found that they give a consistant account of the energy variations of the volume integrals of the optical model potentials. These energy variations are largely determined by the behaviour of the imaginary potential W(E,r) at low energies, in particular by its rapid decrease near the Coulomb barrier.

*Permanent Address: Department of Physics, Aligarh Muslim University, Aligarh, UP, India

0323-0465/94

The absolute magnitude of the dispersion integral, however, depends rather critically on the assumed behaviour of W(E,r) at high energies. Mahaux et al therefore normalised their calculated values to the empirical value of the real volume integral at the maximum.

While the use of volume integrals (as in ref. [2]) is simple and convenient it fails to reveal the radial variation of the dispersion contribution which may be significantly different from that of the mainly energy independent part of the real pontial. This has not been investigated so far for composite projectiles. In the present work, we therefore studied the energy and radial variation of the dispersion contribution.

In Section 2, we derive a dispersion relation (DR) for the equivalent local optical potential. Application of this to the volume integrals of the alpha-^{40}Ca optical potential shows that the nonlocality of the real potential is negligibly small. However, we find that even a purely local potential with the DR term included gives a stronger energy dependence than required by the experimental data. This difficulty is shown to be intimately related to the uncertainties in the imaginary potential at high energies. Further, we also point out that there are some fundamental difficulties in the use of full dispersion relation for any composite projectile if one tries to go beyond studying the qualitative behaviour of the real potential near Coulomb barrier.

Using the empirical data, we have been able to extract, as described in Section 3, one part of the dispersion integral with much less ambiguity. We show that the dispersion relation gives rise to a real surface term as result of a similar term in the imaginary part of the optical potential. The predicted real surface term is then used (in subsection 3.2) to analyse the alpha-^{40}Ca elastic scattering data from 18 to 100 MeV.

We conclude, in Section 4, that the scattering data is consistent with the real surface dispersion term.

2. The Dispersion Relation for Nucleus-Nucleus Scattering

It has been shown by Mahaux and others [1,2] that the real and imaginary parts of the optical model potential for composite particles satisfy the dispersion relation

$$\begin{aligned} V(E;r,r') &= V_0(r,r') + \frac{P}{\pi}\int_{E_F}^{\infty} \frac{W(E';r,r')dE'}{E'-E} \\ &= V_0 + \Delta V(E) \end{aligned} \tag{1}$$

where V_0 and $\Delta V(E)$ are in general non-local. However, for composite particles the non-locality is expected to be small [4] and therefore it has been previously neglected. Initially we assume V_0 to be non-local, and the imaginary potential to be local [2]. To obtain the equivalent local potential we use the Gaussian model of Perey and Buck [5] for the nonlocality of V_0, namely

$$V_0(r,r') = U_0(\frac{r+r'}{2})(\pi\beta^2)^{-3/2}exp[-(\frac{r-r'}{\beta})^2] \tag{2}$$

where β is the rangle of the nonlocality.

Since the phenomenological potentials are local we identify them with the equivalent local potential

$$U_L(E,r) = V_L(E,r) + iW_L(E,r) \tag{3}$$

Using the relation of Pery and Buck [5] gives

$$\begin{aligned} U_L(E,r) &= U_0 exp[-\alpha(E - U_L(E,r) - V_c(r))] \\ &\quad + \Delta V(E,r) + iW(E,r) \end{aligned} \tag{4}$$

where $V_c(r)$ is the Coulomb potential. Since we apply the above relation to study the alpha-^{40}Ca system for which $\alpha = 0.002MeV^{-1}$ ($\alpha = M\beta^2/2\hbar^2$ and $\beta = 0.2fm$ for alpha particles [6]) and the imaginary potential [7] $W_L(E,r) < 30MeV$ for $E < 150MeV$ we expect $\alpha W(E,r)$ to be very small. Using this approximation, the real and imaginary parts of eq.(4) become

$$V_L(E,r) = U_0 exp[-\alpha(E - V_L(E,r) - V_c(r))] + \Delta V(E,r) \tag{5}$$

$$W_L(E,r)[1 - \alpha U_0)(r) exp(-\alpha(E - V_L(E,r) - V_c(r)))] = W(E,r) \tag{6}$$

In order to study the scattering of alpha-particles from ^{40}Ca we make certain simplifying assumptions in eq.(5) as used by Lipperheide and Schmidt [8] for inicident protons. We replace the quatities in the exponentials by their values at $r = 0$ and approximating $V_L(E,0)$ by its empirical value found by Delbar et al [7]

$$V_L(E,0) = -198.6(1 - 0.00168E) \tag{7}$$

and $V_c(0)$ was calculated assuming a uniform spherical charge distribution for ^{40}Ca and a structure less point alpha-particle.

In case of heavy-ion scattering the potential is well determined only at the strong absortion radius (SAR), so eq.(5) has been used at SAR [2,9] with $\alpha = 0.0$, that is a purely local potential. However, ^{40}Ca shows some transparency [9] to alpha-particles and the scattering seems to determine the optical potential even at small radii. After integration over the target volume, eq.(5) becomes

$$J_{V_L}(E) = J_{U_0} exp[-\alpha(E - V_L(E,0) - V_c(0))] + \Delta J_V(E) \tag{8}$$

where

$$J_{V_L}(E) = -\frac{4\pi}{A_P A_T}\int_0^{\infty} V_L(E,r)r^2 dr$$

$$\Delta J_V(E) = -\frac{4\pi}{A_P A_T}\int_0^{\infty} \Delta V(E,r)r^2 dr$$

$$J_{U_0} = -\frac{4\pi}{A_P A_T}\int_0^{\infty} W_L(E,r)r^2 dr$$

$$J_{W_L}(E) = -\frac{4\pi}{A_P A_T}\int_0^\infty W_L(E,r)r^2\mathrm{d}r$$

Since α is quite small, we take $W_L(E) \simeq W(E)$; this simplifies the calculation of the dispersion term in eq(5) without much error and is justified by the scatter of the real volume integrals (see Fig.2). The dispersion term in eq.(8) then becomes

$$\triangle J_V(E) = \frac{P}{\pi}\int_0^\infty \frac{J_{W_L}(E')\mathrm{d}E'}{E'-E} \qquad (9)$$

One difficulty in calculating $\triangle J_V(E)$ using eq.(9) comes from the behavior of $W_L(E)$ at high energies. We have assumed that $W_L(E)$ falls to zero at some cut-off energy E_m as in ref.(2). Our calculations show that although the energy dependence of $J_V(E)$ at low energies does not depend sensitively on the cut-off energy E_m the absolute magnitude of $\triangle J_V(E)$ is quite a sensitive function of E_m. The calculated energy dependence of the dispersion contribution has been extensively used to explain the behaviour of the real potential at energies near the Coulomb barrier [2]. However, the aim of the present study is to estimate the quantitave features of the dispersion relation(eq.(8) and eq.(9)) and to estimate the nonlocality in the real potential for the alpha-^{40}Ca system. This system is chosen because a large body of elastic scattering data is avaible and also ^{40}Ca shows some transparency to alpha-particles for quite small radii, so that the volume integrals of the coresponding potentials are more accurately known than for other systems. The volume integrals of the empirical total imaginary potentials obtained in a large number of previous analyses from 18 to 166 MeV are shown in Figure 1. Following [2] we calculate the dispersion term, approximating $J_{W_L}(E)$ by three straight line segments. The first segment is from imating $J_{W_L}(E)$ by three straight line segments. The first segment is from zero to 72 MeV (where $J_{W_L}(72) = MeV - fm^3$). From 72 MeV to 250 MeV zero to 72 MeV (where $J_{W_L}(72) = 98MeV - fm^3$). From $72MeV$ to 250 MeV we assume a small positive slope so that J_{W_L}=$115MeV - fm^3$ at 250 MeV. This has been found necessary by Mahaux et al to improve agreement with the empirical volume integrals of the real part beyond 80 MeV. Above 250 MeV we take line segments going to zero at 600, 1000 and 5000 MeV to study the effect of these choices on $\triangle J_{V_L}(E)$.

The above form for $J_{W_L}(E)$ allows the volume integral in eq.(9) to be easily evaluated, and using J_{U_0} and α as free parameters we fitted eq.(8) to the empirical real volume integrals, taking $E_m = 1000MeV$. Fig.2 shows that the qualitative features of the energy variation of the real volume integral are reproduced by this calculation. Furthermore our results show that the data reproduced by this calculation. Furthermore our results show that the data require $\alpha = 0.0$ namely a purely local real potential. Setting $\alpha = 0.002MeV^{-1}$ worsens the agreement with the empirical real volume integrals for $E > 80MeV$. Even with a purely local potential the calculated energy dependence is stronger than required by the data. A similar result was found by Mahaux et al [2]. However, here we investigate this discrepency further and estimate the depth of the energy independent term U_0 following the procedure of ref.[8]. Choosing $r_0 = 1.41fm$ and $a_0 = 1.24fm$ (as in ref.7, for which $J_{U_0} = 2.1fm^3$) we find $U_0 = 110MeV$, which is much smaller [4] than four times 70 MeV estimated by Perey and Buck [5] for nucleons.

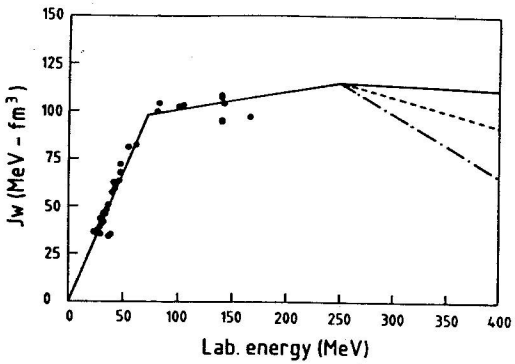

Fig. 1. Solid circles are the volume integrals of imaginary optical potentials [1] from the analyses of alpha-^{40}Ca elastic cross-sections. The three line segments, solid, dashed and dot-dashed, correspond to three cut-off energies E_m = 5000, 1000, 600 MeV.

Table 1. Best fit parameters for $\alpha-^{40}$Ca (see text for details). All depths are in MeV and distances are in fm. D indicates parameters of Potential B from ref. [7].

E [MeV]	V_0	r_0	a_0	W_v	r_w	a_w	W_d	r_d	a_d	$\frac{\chi^2_\sigma}{N_\sigma}$	$\frac{\chi^2_\sigma}{N_\sigma(D)}$
18.0	194.94	1.36	1.35	1.73	2.13	0.30	23.10	1.33	0.32	30	170
22.0	192.15	1.35	1.31	1.65	2.19	0.35	14.80	1.33	0.42	62	143
23.0	185.11	1.38	1.27	0.0	-	-	7.20	1.81	0.55	69	244
24.1	194.31	1.34	1.27	2.03	2.36	0.82	14.47	1.33	0.42	62	143
26.1	177.17	1.41	1.24	5.66	1.79	1.00	11.94	1.33	0.55	90	251
29.0	157.59	1.50	1.17	0.32	2.78	0.34	37.48	1.33	0.47	61	59
36.2	180.97	1.41	1.30	6.58	1.98	1.44	14.69	1.31	0.35	66	85
39.6	175.80	1.39	1.26	12.00	1.65	1.90	14.84	1.43	0.35	47	67
42.6	186.51	1.37	1.30	8.76	1.94	0.57	10.00	1.33	0.35	76	90
49.5	176.41	1.41	1.31	9.70	2.01	0.80	7.00	1.33	0.35	47	63
61.0	157.05	1.41	1.17	19.12	1.72	1.09	4.00	1.33	0.35	14	30
100.0	158.44	1.41	1.22	21.62	1.82	0.83	2.28	1.33	0.35	22	30

Even for $\alpha = 0.002MeV^{-1}$ the calculated depth is only about $174MeV$. Further, the depth U_0 would decrease for a higher cut-off value E_m.

The calculated dispersion term with the high energy cut-offs E_m = 600, 1000 and 5000 MeV are shown in the lower portion of Figure 2. It is notable that although the energy dependence of the dispersion term is very similar (at low energies) in all cases the absolute magnitude increase with increase in cut-off energy. This implies a change in the magnitude of the energy independent term required to match the empirical real volume integrals. Thus the depth U_0 calculated above cannot be extracted unambigously as long as there is uncertainty in the high energy behaviour of the imaginary potential. Further, any increase in the imaginary potential at intermediate energies (as in figure 1 of ref.[10]) would also affect the real potential at high energies (E> $80MeV$). The agreement

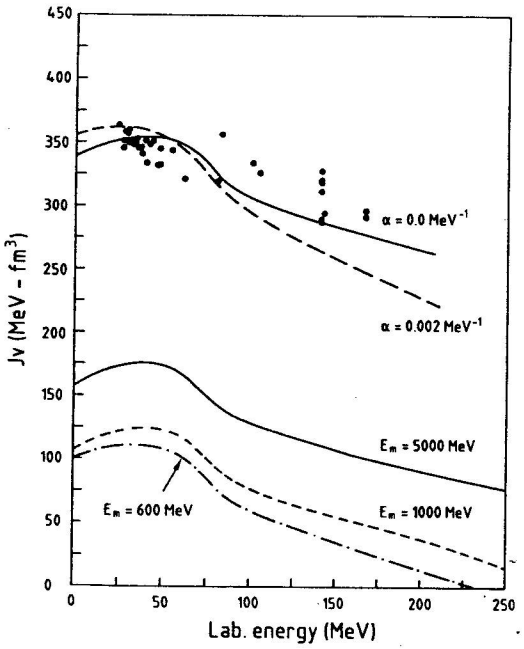

Fig. 2. The three curves in the lower portion of the figure show the dispersion contribution to real volume integrals corresponding to three cutoff values used for J_W compared with volume integrals as in figure 1. The upper portion of the figure shows the empirical (solid circles) and the calculated total volume integral for two values of the non-locality parameter ($E_m = 1000$ MeV used).

obtained by Lipperheide and Schmidt [8] for incident protons depends sensitively on the cut-off energy ($E_m = 600 MeV$,which is quite arbitrary). A higher cutt-off (Fig.1b of ref.[8]) would have resulted in a smaller depth U_0.

The above discussion shows that for composite projectiles the dispersion relation can be used only to study the qualitative features at low a energies. Our calculations show that the absolute magnitude of the dispersion contribution depends quite sensitively on the value chosen for the cut-off energy E_m. Further if the imaginary potential increases in the intermadiate energy region it would also effect the energy dependence of the real dispersion term. Thus there seems to be some real difficulty in the use of full dispersion relation for composite projectiles which would require a rigorous derivation of the corresponding dispersion relation and a better understanding of the asymptotic behaviour of the imaginary potential. The situation is different for incident nucleons, where the dispersion relation is on a much firmer theoretical footing, the particle and hole structure of the target is better known and the high energy behaviour of the

Table 2. Parameters obtained in the modified analysis (see text for details). All depths are in MeV and distance are in fm. * denotes parameter kept fixed during search. D indicates parameters of Potential B from ref.[7]. The + sign denotes attraction and -sign repulsion.

E(MeV)	V_0	ΔV_{dis}	W_d	W_v	r_0	a_0	κ_σ^2/N_σ
18.00	174.71	-	0.0	9.971	D	D	37
	174.81	-	3.55*	8.524	1.41	1.21	38
	165.68	+11.88	3.55*	8.419	1.41	1.23	34
22.00	176.73	-	3.97	9.291	D	D	107
	175.88	-	9.63*	6.85	1.411	1.218	110
	155.75	+13.63	9.63*	6.76	1.45	1.19	106
23.00	173.59	-	11.812	1.307	D	D	76
	173.55	-	11.61*	1.40	1.41	1.21	76
	153.61	+13.41	11.61*	1.35	1.45	1.18	73
24.10	177.44	-	0.0	10.59	D	D	84
	171.23	-	13.86*	5.91	1.408	1.30	96
	171.18	+12.73	13.86*	5.46	1.38	1.36	86
26.13	174.34	-	12.755	7.523	D	D	51
	177.35	-	17.60*	5.66	1.405	1.24	86
	185.07	+10.40	17.60*	4.85	1.352	1.305	62
29.00	174.25	-	25.869	3.134	D	D	51
	172.28	-	21.56*	3.90	1.40	1.21	50
	193.81	+3.92	21.56*	3.67	1.33	1.33	36
33.82	175.12	-	17.095	1.19	D	D	80
	171.07	-	19.42*	0.114	1.405	1.202	72
	217.70	-8.11	19.42*	0.230	1.286	1.34	60
36.20	172.89	-	12.292	10.334	D	D	62
	222.89	-	15.20*	10.00	1.401	1.152	67
	214.12	-11.86	15.20*	8.94	1.31	1.32	56
39.60	173.58	-	5.25	13.44	D	D	42
	175.74	-	8.61*	12.887	1.409	1.258	41
	207.00	-13.40	8.61*	12.743	1.342	1.317	40
42.60	171.26	-	10.23	12.90	D	D	78
	178.36	-	4.21*	14.01	1.387	1.27	76
	256.93	-12.93	4.21*	12.57	1.20	1.441	44
49.50	169.64	-	0.0	16.21	D	D	78
	173.95	-	0.39*	17.01	1.409	1.284	40
	198.76	-7.38	0.39*	16.783	1.347	1.345	39
61.00	166.42	-	3.90	18.49	D	D	20
	165.17	-	0.007*	18.52	1.407	1.224	20
	186.95	-4.04	0.007*	18.52	1.349	1.293	20
100.0	154.14	-	0.0	24.12	D	D	35
	157.54	-	0.0*	24.12	1.402	1.256	34
	172.07	-1.67	0.0*	23.51	1.36	1.31	32

imaginary potential is also more accurately known. However, in the next section we use the empirical imaginary potential to calculate one part of the dispersion integral and also investigate its effect on the elastic angular distribution of alpha-particles by ^{40}Ca.

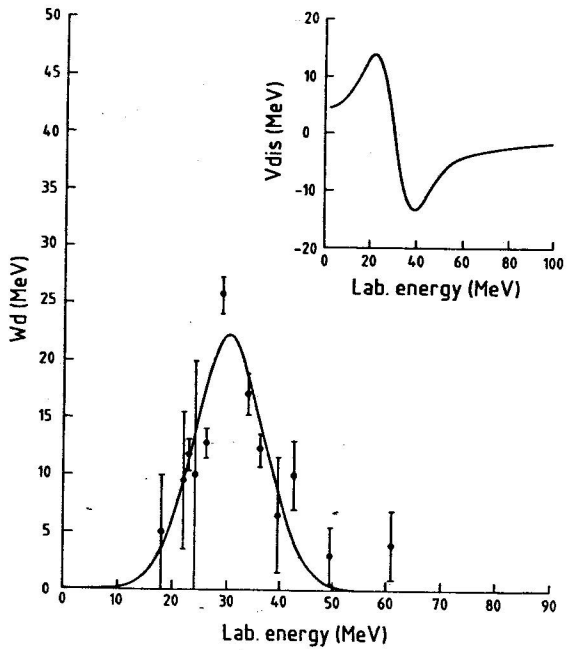

Fig. 3. The depths of the surface imaginary potential for alpha-^{40}Ca found in our analysis. Solid curve represents least square fit using eq. (14). The inset shows the calculated depth of the dispersion contribution eq. (15) using the solid curve for W_d.

3. Dispersion Relation Analysis of Alpha - ^{40}Ca Elastic Scaterring

3.1. The Real Surface Term in the Dispersion Integral

Optical model analyses [7,11] of the elastic scattering of alpha- ^{40}Ca and ^{58}Ni indicate that the imaginary part of the optical model potential can be written as a sum of volume (W_v) and surface derivate (W_d) terms. Furthermore, phenomenological potentials require that the surface imaginary term goes to zero at high energies. We use this empirical fact to calculate the dispersion contribution from the surface term alone and are thus able to avoid the uncertainty connected with the high energy behaviour of the total imaginary potential. We may thus write, using equations (1) and (4), the local optical potential $U_L(E,r)$ in the following form:

$$\begin{aligned} U_L(E,r) &= V_0 + \frac{P}{\pi}\int_0^\infty \frac{[W_v(E',r)+W_d(E',r)]\mathrm{d}E'}{E'-E} \\ &\quad +iW_v(E,r)+iW_d(E,r) \end{aligned}$$

$$\begin{aligned} &= V(E,r)+\frac{P}{\pi}\int_0^\infty \frac{W_d(E',r)\mathrm{d}E'}{E'-E} \\ &\quad +iW_v(E,r)+iW_d(E,r) \\ &= V(E,r)+\Delta V_d(E,r)+iW_v(E,r)+iW_d(E,r) \end{aligned} \tag{10}$$

In these equations we have combined the dispersion contribution from the volume term (W_v) with the energy independent term $V_0(r)$. This helps us to identify $V(E,r)$ with the energy-dependent volume type real potential used phenomenologically. Thus the use of dispersion relation gives rise to a surface real contribution $\Delta V_d(E,r)$ as a consequence of a surface-peaked imaginary potential. Another source of real surface peaking through the dispersion relation would be the increase in imaginary radius with energy. However the latter source would be plagued with the same uncertainties as the imaginary part at high energies. Therefore, we consider here the former source only. A similar type of surface term was predicted [1,12] in the nucleon optical potential. In the next subsection 3.2 we test for the presence of the predicted real surface term by analysing the differential elastic cross-section for alpha-^{40}Ca scattering.

3.2. Analysis of alpha-^{40}Ca Elastic Scattering

In order to test the prediction of real surface term $\Delta V_d(E,r)$, we need to know the energy and radial dependence of $W_d(E,r)$ as unambigously as possible. To achieve this we use the results of earlier analyses [7,13,14] of alpha-^{40}Ca scattering in the energy range from 18 to 166 MeV and adopt the following procedure.

We use the same data as analysed by Delbar at al [7], augmented by those of Gubler et al [13] and the low energy data of Gaul et al [14] at [18] and 22 MeV. The first authors found good overall agreement with the data from 24 to 166 MeV with fixed form factors and potentials depths with the following simple energy variations

$$V_0 = A_1 + A_2E \tag{11}$$

$$W_v = A_2 - A_3\exp(-A_4E) \tag{12}$$

$$W_d = A_5\exp(-A_6E) + A_7 \tag{13}$$

with squared Saxon-Woods form factors for V_0 and W_v and the derivative of this for W_d. The values of chi-squares corresponding to the potential of ref. [7] are listed in the last column of Table 1. Fig. 1 of ref. [7] and Table 1 show that the fits deteriorate at lower energies. Since the effects of the dispersion term $\Delta V_d(E,r)$ (see Figure 3) are greater at low energies, one of the objects of the present work was to see if the fits at the lower energies could be improved by the inclusion of the real surface dispersion term without introducing additional parameters. It is notable, that the values of some of the parameters (in ref. [7]) might be considered somewhat unphysical, in particular the high value of the radius parameter r_w and the low value of r_d, and we wanted to see if this could be improved without significant reduction in the quality of agreement.

The whole data were therefore reanalysed allowing all parameters to vary, starting from the Delbar values except for those considered unphysical. In particular, the value

of r_d was initially fixed to 1.33fm, and allowed to vary only in the final stages of the fitting procedure. The results are shown in Table 1, and it is notable that although the form factors are now much more reasonable, the values of the depths show such large fluctuations with energy that it is difficult to use them in the dispersion integral. Furthermore, the quality of agreement is in most cases not significantly better than those of Delbar, although the chi-square values in Table 1 refer to an average smoothly varying potential, whereas in our analysis all the parameters were varied at each energy. We therefore adopted the form factors of Delbar in our subsequent calculations.

In the first of these, the potential depths V_0, W_d and W_v were varied, keeping the form factors fixed to the Delbar values $r_0 = 1.41$fm, $a_0 = 1.24$fm, $r_d = 0.62$fm, $a_d = 1.04$fm, $r_w = 1.79$fm and $a_w = 1.00$fm. The results are shown in the first line of Table 2 for each energy. To allow for the possibility that the average geometry of the real potential may not be sufficiently flexible to absorb the effect of the energy-varying dispersion term, the analysis was repeated allowing r_0 and a_0 to vary also. The optimum values found for these parameters, together with the corresponding values of chi-squares, are given in the next line in Table 2.

The energy dependence of the surface imaginary potential depth W_d found in this analysis are shown in Fig. 3. The error bars show the range of depths which cause a less than 20 % increase of chi-square. It was found necessary to smooth any abrupt changes of W_d with energy at few energies only. Since the functional form for $W_d(E)$ used by Delbar et al increases exponentially at lower energies, we used the form

$$W_d(E) = x_1(E - x_2)\exp(-((E - x_3)/x_4)^2) \tag{14}$$

where x_1, x_2, x_3 and x_4 are varied to optimise fit to the depths shown in Fig. 3 in the energy range from 18 to 61 MeV. Equation (15) thus represent the average energy variation of the surface imaginary potential depth $W_d(E)$. Since the surface part of the imaginary potential is not well determined [14] at low energies ($E < 18$ MeV) we use a line segment from 0 to 10 MeV to calculate the dispersion term $V_d(E, r)$. This introduces some uncertainty in the dispersion integral but we feel that this approximation is justified given the exploratory nature of the present work. Using this prescription for the energy dependence of $W_d(E, r)$, we evaluated the dispersion integral

$$\Delta V_d(E, r) = \Delta V_{dis}(E)g(r) = \frac{P}{\pi}\int_0^\infty \frac{W_d(E', r)\mathrm{d}E'}{E' - E} \tag{15}$$

and the resulting depths of the real surface term are shown as inset in fig. 3. The radial variation $g(r)$ of the $\Delta V_d(E, r)$ is identical to that of $W_d(E, r)$ used in ref. [7].

Having fixed $W_d(E, r)$ the calculated $\Delta V_d(E, r)$ was then added to the real potential used in the earlier analysis. The alpha-^{40}Ca elastic angular distribution was then reanalysed in the energy range $18 < E < 100$ MeV with the modified real potential. To obtain the best fit to the data only four parameters were allowed to vary, the imaginary volume depth W_v and the three parameters V_0, r_0 and a_0 of the volume real potential. The surface imaginary depths were held fixed to the values obtained by fitting eq. (15) to the empirical depths, so that the additional real dispersive term is consistant with the imaginary potential $W_d(E, r)$ used. Thus the number of parameters in our analysis

is the same as in the phenomenological analysis and hence a comparision of the corresponding chi-squares may be made. The results are shown in the last line for each energy in Table 2. Table 2 shows that at almost every energy the value of chi-square is lowered by the inclusion of the real surface term calculated from the dispersion relation, although the reduction is not significant. This surface term should not be confused with the purely phenomenological real surface term used in ref. [15].

5. Conclusions

We have shown that the low energy alpha-^{40}Ca elastic scattering data is qualitatively consistent with the dispersion relation. The behaviour of the real volume integrals near Coulumb barrier in nicely reproduced by the DR. However, the energy dependence of the real volume integral beyond 80 MeV is more than required by the empirical data. Any nonlocality present in the real potential has been shown to worsen this disagreement. This difficulty, also found earlier, has been shown to be intimately related with the ambiguities in the high energy behaviour of the imaginary potential. Further, our results suggest that there are real difficulties in the use of full DR which require further theoretical efforts.

To avoid the above difficulty we have successfully used the empirical result that the surface type of imaginary potential vanishes at high energies. The surface imaginary potential has been shown to give rise to a real surface term through the DR. Our calculations show that this surface real term is attractive below 30 MeV, repulsive beyond 30 MeV and vanishes at high energies. We have been able successfully to account the alpha-^{40}Ca elastic scattering data in the energy region $18 < E < 100$ MeV with this additional real surface term without any additional parameters. Our analysis indicates an iterative procedure: Using the empirical $W_d(E)$ to calculate $\Delta V_d(E)$, add the calculated $\Delta V_d(E)$, varying $W_d(E)$ would then redetermine $\Delta V_d(E)$. We have performed the first cycle of this iteration to show that the elastic scattering data is consistent with the DR real surface term. Further cycles were not attempted since we feel that the radius parameter of the surface imaginary potential, $r_d = 0.62$fm, is too small and the uncertainties in the imaginary potential at low energies are difficult to remove. Our results suggest a reanalysis of the alpha-^{59}Ni data where the empirical analysis indicate a strong surface imaginary potential at low energies.

One of us (W.H.) acknowledges the award of a SERC Visiting Fellowship that enabled him to spend a year at Oxford. We are grateful to Dr. J.R. Rook for many useful discussions and suggestions. W.H. also thanks Prof. I. Ahmad for introducing him to the dispersion relation technique.

References

[1] C. Mahaux, H. Ngo: *Nucl. Phys.* **A378** (1982), 205; and references therein; P.E. Hodgson: *Proc. Int. Conf. Nucl. Reactions, Calcutta 1989, World Scientific* (1989), 39; Int. Conf. on Nucl. Data for Science and Technology, Julich (1991): J.P. Delaroche, W. Tornow: *Phys. Lett.* **B203** (1988), 4;

[2] C. Mahaux, H. Ngo, G.R. Satchler: *Nucl. Phys.* **A449** (1986), 354; M.A. Nagarajan, C. Mahaux, G.R. Satchler: *Phys. Rev. Lett.* **54** (1985), 1136;
[3] A.C. Merchant, K.F. Pal, P.E. Hodgson: *J. Phys.* **G15** (1989), 601;
[4] D.F. Jackson, R.C. Johnson: *Phys. Lett.* **B49** (1974), 249;
[5] F.G. Perey, B. Buck: *Nucl. Phys.* **32** (1962), 353;
[6] P.P. Singh, P. Schwandt, G.C. Yang: *Phys. Lett.* **B59** (1975), 113;
[7] Th. Delbar, Gh. Gregoire, G. Paic, R. Ceuleneer, F. Michel, R. Vanderpoorten, A. Budzanowski, H. Dabrowski, L. Friendl, K. Grotowski, S. Micek, R. Planeta, A. Strzałkowski, K.A. Eberhard: *Phys. Rev.* **C18** (1978), 1237;
[8] R. Lipperheide, A.K. Schmidt: *Nucl. Phys.* **A112** (1968), 65;
[9] G.R. Satchler: *Direct Nuclear Reactions* (Oxford, 1983);
[10] G. Passatore: *Nucl. Phys.* **A110** (1968), 91;
[11] A. Budzanowski, H. Dabrowski, L. Friendl, K. Grotowski, S. Micek: *Phys. Rev.* **C17** (1978), 951;
[12] I. Ahmad, W. Haider: *J. Phys.* **G2** (1976), L157;
[13] H.P. Gubler, U. Kiebele, H.O. Meyer, G.R. Plattner, I. Sick: *Nucl. Phys.* **A351** (1981), 29;
[14] G. Gaul, H. Ludecke, R. Santo, H. Schmeing, R. Stock: *Nucl. Phys.* **A137** (1969), 177;
[15] C.P. Robinson, J.P. Aldridge, R.H. Davis: *Phys. Rev.* **171** (1968), 1241; J. John, C.P. Robinson, J.P. Aldridge, R.H. Davis: *Phys. Rev.* **177** (1969), 1755;
[16] A.M. Kobos, G.R. Satchler, R.S. Mackintosh: *Nucl. Phys* **A395** (1983); 248;